Available online at www.sciencedirect.com
SCIENCE DIRECT
Physics Letters A 354 (2006) 472–476
PHYSICS LETTERS A
www.elsevier.com/locate/pla

Magnetization steps in the phase separated manganite $La_{0.275}Pr_{0.35}Ca_{0.375}MnO_3$

B.C. Zhao *, Y.Q. Ma, W.H. Song, Y.P. Sun *

Key Laboratory of Materials Physics, Institute of Solid State Physics, Chinese Academy of Sciences, Hefei 230031, China

Received 25 July 2005; accepted 20 January 2006

Available online 10 February 2006

Communicated by J. Flouquet

Abstract

The low temperature magnetic properties of the $La_{0.275}Pr_{0.35}Ca_{0.375}MnO_3$ manganite have been investigated. Step-like charge ordered antiferromagnetic (AFM)–ferromagnetic (FM) transition is observed in the magnetic field dependence of magnetization $M(H)$ curve below 200 K as the applied magnetic field is only several Tesla, and the magnetic step become ultrasharp at 2 K. The onset magnetic field of the step decreases initially and then increases with increasing temperatures and the critical magnetic field is sensitive to the magnetic history. The results are discussed according to the field-induced reduction of the distortion of Mn–O octahedron as martensitic mechanism. The magnetic phase diagram is also constructed based on the magnetic measurements.

PACS: 75.60.Ej; 75.80.+q; 81.30.Kf

Keywords: Magnetic step; Phase separation

1. Introduction

The recent studies of the colossal magnetoresistance (CMR) in the perovskite manganites have shown that these materials exhibit complex phenomena of phase separation (PS) and charge ordering (CO) or orbital ordering (OO) [1–3]. The PS scenario fully develops in the $La_{5/8-y}Pr_yCa_{3/8}MnO_3$ system of compounds, whose end members exhibit homogenous ferromagnetic (FM) ($y = 0$) and CO ($y = 1$) states [4]. The ground state of the immediate compounds is imhomogenous due to the coexistence of CO antiferromagnetic (COAFM) and FM phases [5]. The nature of the Jahn–Teller (JT) Mn^{3+} cations is responsible for the strong coupling between charge, spin and the lattice and then the ground state in these materials [6]. The subtle balance of these separated phases can be manipulated by exerting an external stimulus, such as magnetic field, electric field, pressure, and illumination with light or X-ray, etc.

Recently, an interesting phenomenon has been found in the phase separated manganites, that is, the appearance of ultrasharp magnetization steps at low temperatures (below ∼5 K) in the virgin isothermal magnetization $M(H)$ curves and the magnetization steps are sensitive to the magnetization history [7,8]. The step-like behaviors were also observed in resistivity and specific heat measurements. The origin of these phenomena is still a matter of controversy. Various models have been proposed to interpret the complex magnetization steps at low temperatures in manganites, such as martensitic transformation scenario [9], quenched disorder induced magnetization jump [10], spin reorientation [11,12], and so on. Among these interpretations, the martensitic scenario is attracting considerable attention. In the martensitic model, there exists a strain effect at the interface of COAFM and FM domains in the doped PS manganites. At low temperatures, the driving force of the applied magnetic field overcomes the elastic energy due to the interfacial constraints. For a critical value of the applied magnetic field, the local stress is released and the magnetization step appears. However, the martensitic scenario cannot explain all phenomena of the magnetization steps such as the multiple

* Corresponding authors.
E-mail addresses: bchzhao@issp.ac.cn (B.C. Zhao), ypsun@issp.ac.cn (Y.P. Sun).

0375-9601/$ – see front matter
doi:10.1016/j.physleta.2006.01.088

steps in the $M(H)$ curves. In order to further understand the origin of the step-like magnetic transition in the doped manganites, we carefully investigated the magnetic properties in a polycrystalline $La_{0.275}Pr_{0.35}Ca_{0.375}MnO_3$ manganite.

2. Experiment

Polycrystalline $La_{0.275}Pr_{0.35}Ca_{0.375}MnO_3$ sample was prepared through the conventional solid-state reaction method in air [13]. Appropriate proportions of high purity La_2O_3, Pr_6O_{11}, $CaCO_3$, and MnO_2 powders were thoroughly mixed according to the desired stoichiometry, and then prefired at 1000 °C for 24 h. The powders obtained were ground, pelletized, and calcined at 1200 °C for 24 h with intermediate grinding. and finally, sintered at 1400 °C for 24 h and slow-cooled to room temperature. Phase purity and the structure of the sample were studied using powder X-ray diffraction (XRD) with Cu K_α radiation at room temperature. The magnetic measurements were performed on a superconducting quantum interference device (SQUID) MPMS system ($2\ \mathrm{K} \leqslant T \leqslant 400\ \mathrm{K}$, $0\ \mathrm{T} \leqslant H \leqslant 5\ \mathrm{T}$).

3. Results and discussion

Fig. 1 shows the temperature dependence of magnetization M for the $La_{0.275}Pr_{0.35}Ca_{0.375}MnO_3$ sample in the temperature range of 5–300 K. The data were taken on the heating process under applied fields of 0.01, 0.2, 1, 2, 3 and 5 T after the sample were both zero-field cooled (ZFC) and field cooled (FC) from 300 K. The magnifying $M(T)$ curve under the applied magnetic field of 0.2 T in the temperature region of 130–250 K is displayed in the inset of Fig. 1, implying that there exist two cusps in the $M(T)$ curve under 0.2 T field around 202 and 166 K, which are the CO transition temperature (defined as T_{CO}) and the AFM transition Néel temperature (defined as T_N), respectively. T_{CO} is not almost affected by the low applied field below 1 T. However, as the magnetic field $\mu_0 H \geqslant 3$ T, the COAFM state can be melted into FM state. As the temperature

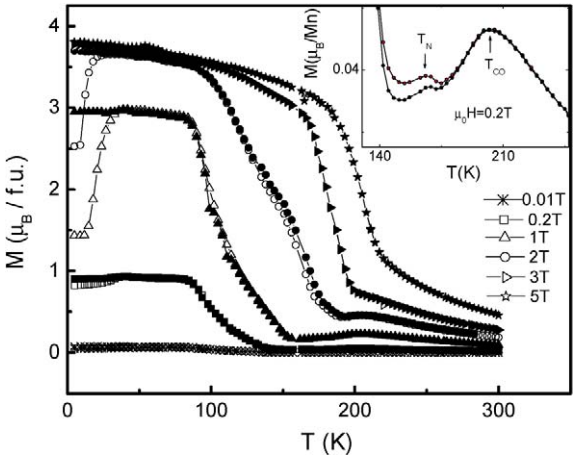

Fig. 1. Temperature dependence of magnetization measured at 0.01, 0.2, 1, 2, 3 and 5 T for $La_{0.275}Pr_{0.35}Ca_{0.375}MnO_3$. The open symbols represent the ZFC data and the filled symbols denote the FC data. The inset shows the magnified $M(T)$ plot around T_N at 0.2 T.

is decreased further, the $M(T)$ curve shows a sharp upturn at a certain temperature T_C, implying that the appearance of FM state. That is to say, there exist competing phases of COAFM and FM at low temperatures in $La_{0.275}Pr_{0.35}Ca_{0.375}MnO_3$ manganite. The competition between FM and AFM exchange interaction leads to the appearance of the spin glass (SG) or cluster glass (CG) state, which can be further proved by the deviation between the ZFC and FC magnetization curves under the lower magnetic field ($\leqslant 2$ T) below a certain temperature T_{irr}. T_{irr} shifts to lower temperatures as the applied field increases, which is a typical character of the glass state. The SG or CG state at low temperatures transfers to a full FM state under enough high magnetic fields ($H \geqslant 3$ T).

In order to further investigate the difference of FC and ZFC, the temperature dependence of the irreversible magnetization $M_{irr} = M_{FC} - M_{ZFC}$ under several applied magnetic fields are plotted in Fig. 2. M_{irr} shows a negative value under the low magnetic field ($\leqslant 1$ T) in a certain temperature region. This unusual feature may be related to the large magnetostriction present in this material [14]. The mechanism of magnetostriction originates from the interchange coupling of magnetic moment of atoms in the sample. The onset temperature of magnetostriction decreases and the temperature region where the magnetostriction exists increases with increasing magnetic field when the applied field $\mu_0 H \leqslant 1$ T. However, the phenomenon of magnetostriction disappears as the applied magnetic field $\mu_0 H \geqslant 2$ T, implying that the magnetostriction forms in a low magnetic field and is suppressed by a higher magnetic field. A Curie–Weiss (CW) fit is also performed in high temperature paramagnetic (PM) phase of $La_{0.275}Pr_{0.35}Ca_{0.375}MnO_3$, which gives the Weiss temperature $\Theta = 186.2$ K and the effective magnetic moment $\mu_{eff} = 4.88\mu_B$/f.u., the latter value is much higher than the theoretical expectation ($\mu_{eff} = 4.54\mu_B$/f.u.). The difference between the experiment and the theory values may be related to the magnetic moment of Pr ions or the FM clusters exist in the high temperature PM phase.

In Figs. 3 and 4, we show the magnetic field dependence of the magnetization, $M(H)$, at a series of selected temperature points. For each measurement, the sample was cooled under zero field from 300 K to the selected temperature and the measurements were performed in a sweeping mode ($0 \to 5\ \mathrm{T} \to 0$). It can be seen that the magnetization M increases almost linearly with increasing magnetic fields in the high temperature region of $T \geqslant 220$ K, which is consistent with the magnetic behavior of PM materials. As $T = 200$ K, M increases almost linearly with the applied magnetic field up to 3.41 T, then the slope of M–H curve increases rapidly as the magnetic field is increased further. According to the M–T data, the sample lies in a CO state at this temperature region. From the increasing slope of the M–H curve, it can be suggested that partial CO states in the sample is melted under stronger magnetic field. However, M still keeps a small value at this temperature even though the magnetic field is up to 5 T, indicating the stronger CO background state under the high magnetic field. In addition, there is almost no hysteresis in the M–H curves, implying the reversible transition between the CO and FM state. From the $M(T)$ data shown in Fig. 1, the sample lies in the COAFM

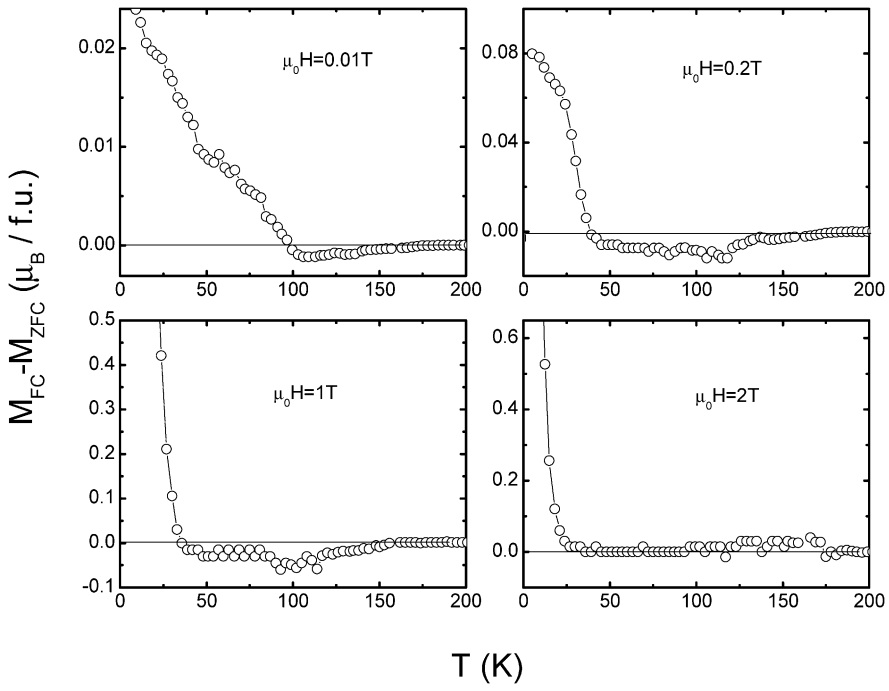

Fig. 2. Temperature dependence of the irreversible magnetization $M_{\rm irr}(= M_{\rm FC} - M_{\rm ZFC})$ in various magnetic fields $\mu_0 H = 0.01$ T (a), 0.2 T (b), 1 T (c) and 2 T (d).

state in the temperature region of 80–180 K. In this temperature region, the initial magnetization increases almost linearly with H as shown in Fig. 4, which reflects the magnetic behavior of AFM phase domains at low magnetic fields. The increased magnetic field can reduce the canting angle of the AFM phase. At a sufficiently high magnetic field $H_{\rm C}$, a field-induced magnetization step appears and the system changes from COAFM to FM state. The magnetization reaches almost a saturated value of magnetic moment at 5 T, the saturation moment increases with decreasing the temperature. As the field decreases, the system does collapse back to the AFM state at a critical field $H'_{\rm C}$, which lower than the corresponding $H_{\rm C}$, meaning the transition between COAFM and FM state has a first-order character [15]. The critical magnetic field $H_{\rm C}$ decreases and the magnetic hysteresis increases with decreasing temperatures in this temperature region, implying that the thermal excitation at a finite temperature region will assist the system to undergo an FM–AFM transition but limit the transition from AFM to FM.

As the temperature is below 60 K, the initial magnetization increases linearly with H up to the critical field $H_{\rm C}$, which is similar to the M–H behavior in the temperature region of 80–180 K. As the magnetic field increases further, a magnetization step in the virgin isothermal M–H curves and the magnetization step brings the system to a full polarized FM state with a saturated magnetic moment of $3.9\mu_{\rm B}$/f.u. The saturated magnetic moment is much higher than the expected one of Mn^{3+} and Mn^{4+} ions, which may be related to the magnetic moment of Pr^{3+} ions in the sample similar to the behavior of the effective magnetic moment $\mu_{\rm eff}$ mentioned above. However, as the magnetic field decreases, the system does not collapse to AFM state but keeps in FM state even when the field is decreased to 0 T, which is inconsistent with the magnetic behavior of the sample in the temperature region of 80–180 K. As it can be

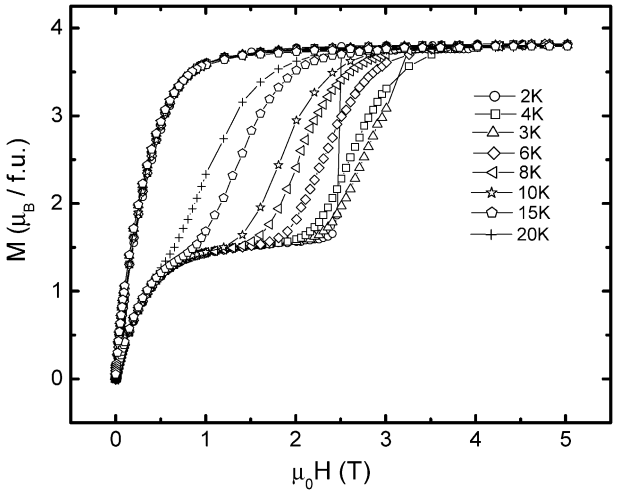

Fig. 3. Field dependence of magnetization in the temperature region of 2–20 K measured in the ZFC mode. The arrows indicate the magnetic field increasing (1) and decreasing (2) branches.

seen from Figs. 3 and 4, the transition from COAFM to FM state shows a successive behavior above 2 K. However, the behavior at 2 K changes dramatically, which shows an abrupt step in the vicinity of 1.65 T. The width of the transition is as small as the limitation of our measurement step 0.05 T. It should be noted that the present compound exhibits a unique sharp transition at low temperatures. Whereas in studies on the A or B site doped $Pr_{1-x}Ca_xMnO_3$ manganite several steps are observed [7,8]. The variation of the number of magnetization steps may be related to the different magnetic ground state in these samples. In addition, except for the ultrasharp magnetization step near 1.65 T, there exists a broader magnetization tail in the vicinity of 3.76 T in the ZFC M–H curve as shown in

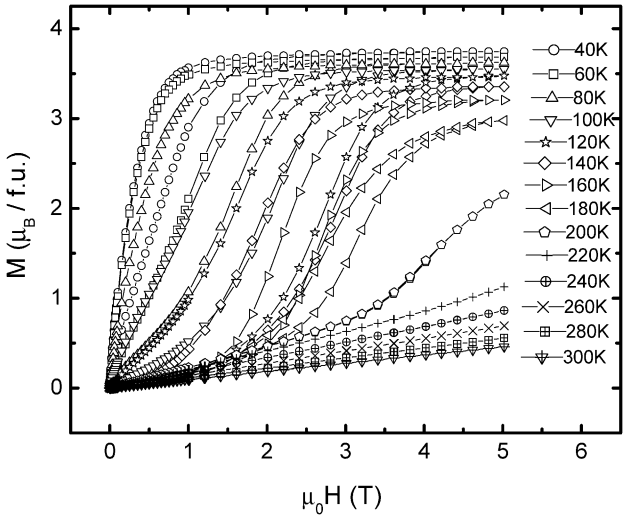

Fig. 4. Field dependence of magnetization in the temperature region of 40–300 K measured in the ZFC mode. The arrows indicate the magnetic field increasing (1) and decreasing (2) branches.

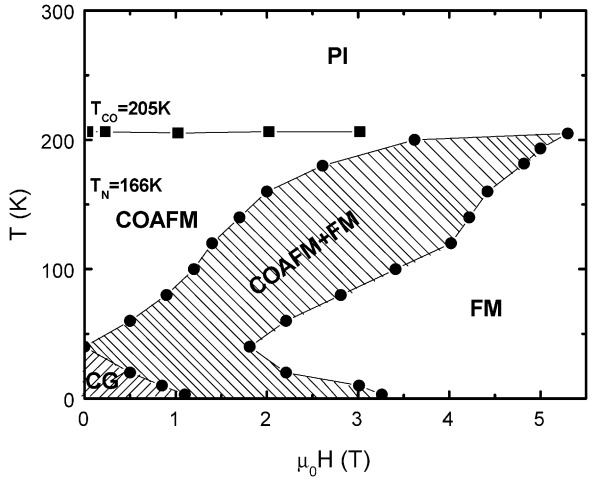

Fig. 5. Magnetic phase diagram of $La_{0.275}Pr_{0.35}Ca_{0.375}MnO_3$. The critical magnetic field was determined by M–H loops at each temperature. T_{CO} under each magnetic field was estimated from $M(T)$ curves. The PI, COAFM, FM, and CG denote the paramagnetic insulating, charge ordered antiferromagnetic, ferromagnetic metals, and cluster glass states, respectively.

the inset of Fig. 6(a), which may be related to the magnetic moment of Pr^{3+} ions. As the magnetic field decreases from 5 T, a full FM behavior is observed. The results show that the sample has a magnetic memory effect.

From the magnetic measurement under various conditions described above, we construct a magnetic phase diagram of $La_{0.275}Pr_{0.35}Ca_{0.375}MnO_3$ as shown in Fig. 5. The critical magnetic field was determined by ZFC $M(H)$ loops at each temperature. T_{CO} and T_N under each magnetic field are estimated in terms of $M(T)$ curves. A striking feature is that COAFM-FM transition is induced by a relatively low magnetic field ∼1.8 T at 40 K. Below 40 K, the FM state is metastable even without magnetic field, which can be elucidated by the SG or CG state as shown in Figs. 1 and 5. The critical magnetic field is a function of temperature both below and above 40 K. Above 40 K,

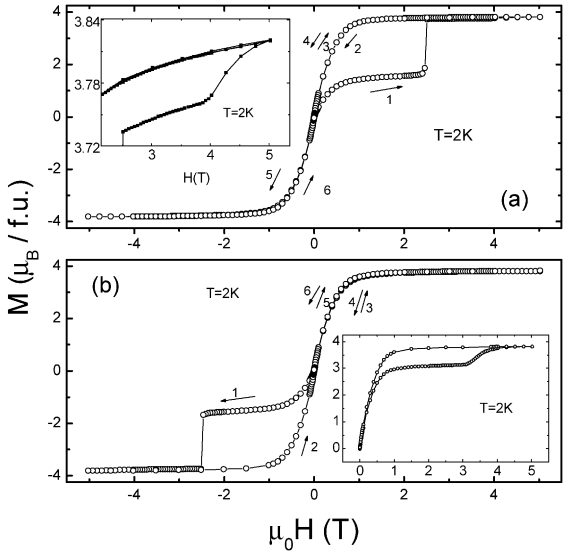

Fig. 6. Isothermal ($T = 2$ K) $M(H)$ curves measured in different changed modes of magnetic field for $La_{0.275}Pr_{0.35}Ca_{0.375}MnO_3$. (a) $0 \to 5$ T $\to 0 \to 5$ T $\to 0 \to -5$ T $\to 0$. The inset shows the second step of the sample. (b) $0 \to -5$ T $\to 0 \to 5$ T $\to 0 \to 5$ T $\to 0$. The inset of (a) shows the ZFC magnetization tail at 2 K. The inset of (b) shows the 1 T FC magnetic step at 2 K.

the critical magnetic field increases with increasing the temperatures, implying a more stable state of COAFM in higher temperature for this material. However, H_C increases with decreasing temperatures below 40 K, which may be related to the enhancement of energy barrier between COAFM and FM as the temperature decreases.

In order to further study the ultrasharp magnetization step observed at 2 K, a series of M–H measurements at 2 K was performed on the sample. The relevant results are shown in Fig. 6 and its inset. Firstly, the sample was FC from 300 K at an applied magnetic field of 1 T and 5 T, after the temperature become stable at 2 K, the field was reduced to zero, and then M–H was measured in a field sweep mode 0–5 T–0. As it can be seen for the 1 T FC data as shown in the inset of Fig. 6(b), the magnetization step becomes considerable broader compared with the ZFC M–H data and the critical magnetic field increases to 3.1 T. The FM phase of the ground state at 2 K (defined as M_{1T}/M_{5T} at 2 K) increases from 37% for the ZFC mode to 81% for the 1 T FC mode. As to the M–H data measured in the 5 T FC condition, the curve displays an almost fully FM state, the magnetization reaches saturation at about 1 T and keeps constant up to 5 T for the sample, which is considered as a result of the rotation of the magnetic domain under external magnetic field. That is to say, the ground state of the sample is FM under the 5 T FC mode condition. Secondly, two separate measurements were performed in order to study the whole M–H behavior of the sample. Before each measurement, the sample was zero-field cooled to 2 K and then the data were collected in field sweeping process of $0 \to 5$ T $\to 0 \to 5$ T $\to 0 \to -5$ T $\to 0$ and $0 \to -5$ T $\to 0 \to 5$ T $\to 0 \to 5$ T $\to 0$. The result is displayed in main panel of Fig. 6. The magnetization step only appears in the virgin branch of the M–H curve for both measurements. Both the second and third cycling curves

display FM behavior. This phenomenon shows that the low temperature magnetic behavior of the sample has the character of memory effect.

The sharp magnetization step at low temperatures in $La_{0.275}Pr_{0.35}Ca_{0.375}MnO_3$ manganite can be explained by the martensitic scenario. Previous studies show that the CO state in $La_{5/8-y}Pr_yCa_{3/8}MnO_3$ belongs to the 1/2-type [3]. The $Mn^{3+}O_6$ Jahn–Teller (JT) distorted octahedral with associated OO are the fundamental building blocks of the COAFM state in $La_{0.275}Pr_{0.35}Ca_{0.375}MnO_3$ manganite. The average radius of A-site cations $\langle r_A \rangle$ for $La_{0.275}Pr_{0.35}Ca_{0.375}MnO_3$ is 1.190 Å [13]. The magnetic properties of CO manganite with moderate $\langle r_A \rangle$ are sensitive to the external disturbance, especially to the magnetic field. According to the Raman experiment [16], the orthorhombic distortions or $Mn^{3+}O_6$ octahedrals can be reduced gradually with increasing magnetic fields. In the case of $La_{0.275}Pr_{0.35}Ca_{0.375}MnO_3$, FM phase competes and coexists with the COAFM phase. The FM regions related to the less distorted $Mn^{3+}O_6$ octahedral have a different symmetry compared with the more distorted COAFM domains. As the magnetic field increases, at low temperatures, the nucleation of the COAFM-FM transformation starts around the regions surrounding the distorted $Mn^{3+}O_6$ octahedral. If the magnetic energy overcomes the elastic strain energy of the distorted $Mn^{3+}O_6$ octahedral, the interface between the more distorted COAFM and FM regions undergoes a sudden motion. The local stress is released and the sharply magnetization step appears.

As to the present compound exhibits only one sharp transition at low temperatures whereas in studies by others several steps are observed, it suggested to be related to the different magnetic ground in these samples. Previous studies on doped $Pr_{1-x}Ca_xMnO_3$ manganite shown that the number of magnetization steps decreases with decreasing stability of the CO structure [8]. In a lightly Ga or Ni-doped manganites, where the CO state is extremely stable, three or four steps are needed to reach a completely FM state whereas only one magnetization jump is observed when the FM is maximum in the Ga-doped series. The FM component is much higher and the CO structure is much instable in the present sample compared to the $Pr_{1-x}Ca_xMnO_3$ series. The CO structure can be easily destroyed by the external disturbance, such as electrical field [13], magnetic field, and so on. Only one magnetization step is sufficient to bring the compound to a full FM state.

4. Conclusion

In summary, we have extensively studied the magnetic properties of $La_{0.275}Pr_{0.35}Ca_{0.375}MnO_3$ manganite. A step-like COAFM–FM transition appears below 200 K and the critical magnetic field decreases initially and then increases with increasing temperatures. The transition becomes ultrasharp as the temperature decrease to 2 K and transition at low temperatures has an irreversible character. The results are discussed in terms of the mechanism of martensitic scenario related to the field-induced reduction of the distortion of Mn–O octahedron.

Acknowledgements

This work was supported by the National Key Research under Contract No. 001CB610604, and the National Nature Science Foundation of China under Contract Nos. 10474100 and 10374033, and the Fundamental Bureau Chinese Academy of Sciences.

References

[1] S. Mori, C.H. Chen, S.-W. Cheong, Phys. Rev. Lett. 81 (1998) 3972.
[2] A. Moreo, S. Yunoki, E. Dogotto, Science 283 (1999) 2034.
[3] M. Vehara, S. Mori, C.H. Chen, S.W. Cheong, Nature (London) 399 (1999) 560.
[4] D. Khomskii, Physica B 280 (2000) 325.
[5] I.G. Deac, S.V. Diaz, B.G. Kim, S.-W. Cheong, P. Schiffer, Phys. Rev. B 65 (2002) 174426.
[6] A.J. Millis, P.B. Littlewood, B.I. Shraiman, Phys. Rev. Lett. 74 (1995) 5144.
[7] R. Mahendiran, A. Maignan, S. Hébert, C. Martin, M. Hervieu, B. Raveau, J.F. Mitchell, P. Schiffer, Phys. Rev. Lett. 89 (2002) 286602.
[8] A. Maignan, S. Hébert, V. Hardy, C. Martin, M. Hervieu, B. Raveau, J. Phys.: Condens. Matter 14 (2002) 11809.
[9] V. Hardy, S. Majumdar, S.J. Crowe, M.R. Lees, D.Mck. Paul, L. Hervé, A. Maignan, S. Hébert, C. Martin, C. Yaicle, M. Hervieu, B. Raveau, Phys. Rev. B 69 (2004) 020407(R).
[10] L.L.M. Fisher, A.V. Kalinov, I.F. Voloshin, N.A. Babushkina, D.I. Khomskii, Y. Zhang, T.T.M. Palstra, Phys. Rev. B 70 (2004) 212411.
[11] G.X. Cao, J.C. Zhang, S.X. Cao, C. Jing, X.C. Shen, Phys. Rev. B 71 (2005) 174414.
[12] G.X. Cao, J.C. Zhang, S.X. Cao, C. Jing, X.C. Shen, Appl. Phys. Lett. 86 (2005) 042507.
[13] Y.Q. Ma, W.H. Song, J.M. Dai, R.L. Zhang, J. Yang, B.C. Zhao, Z.G. Sheng, W.J. Lu, J.J. Du, Y.P. Sun, Phys. Rev. B 70 (2004) 054413.
[14] V. Hardy, A. Maignan, S. Hébert, C. Yaicle, C. Martin, M. Hervieu, M.R. Lees, G. Rowlands, D.Mck. Paul, B. Raveau, Phys. Rev. B 68 (2003) 220402(R).
[15] G. Xiao, E.J. McNiff Jr., G.Q. Gong, A. Gupta, G.L. Canedy, J.Z. Sun, Phys. Rev. B 54 (1996) 6073.
[16] J.M. Li, A.C.H. Huan, Y.W. Du, D. Feng, Z.X. Shen, Phys. Rev. B 63 (2000) 024416.